

Effect of anharmonicity on charge transport in hydrogen-bonded systems

D. Hennig,^{1,2} C. Neißner,¹ M. G. Velarde,¹ and W. Ebeling^{1,2}

¹*Instituto Pluridisciplinar, Universidad Complutense, Paseo Juan XXIII, 1, 28040 Madrid, Spain*

²*Institut für Physik, Humboldt-Universität Berlin, Newtonstrasse 15, 12489 Berlin, Germany*

(Received 20 September 2005; revised manuscript received 28 November 2005; published 30 January 2006)

We study solitonic charge transport in a hydrogen-bonded model system representing a one-dimensional polypeptide chain. Supersonic solitons are constructed for zero temperature in the frame of a Morse lattice model for which an (nonlinear) electronic system is coupled in a tight-binding approximation to H-bond vibrations of the molecular chain. The latter are of anharmonic nature. Charge transport is realized via the coupling between the electron and the local lattice deformations. This electron-lattice coupling is described by the soliton solutions, assigned to states of a localized charge in association with its local chain deformation. By retaining the discrete nature of the underlying lattice system it is shown that even strongly localized states are mobile. In fact, we illustrate that for nonlinear electron-vibration interaction supersonic solitonic carriers in the lattice assist the transport of narrow electron and lattice solitons. Moreover, by using realistic values from polypeptides for the system parameters we demonstrate that the interaction between the H-bond vibrations and the electron is strong enough to sustain thermal perturbations up to $T=300$ K. Most importantly localization is maintained over extended periods of time during which the electron travels directionally over such long distances along the chain exceeding by far those achievable with single-step tunneling. Furthermore, we discuss the role of an applied electric field. It is demonstrated that in a wide range of its values the velocity of the soliton motion and hence the electric current remains unaffected by the electric field. Above this range the velocity of the solitons is proportional to the field strength so that the corresponding current follows Ohm's law. Then for still higher field strengths above a critical value the coupling between electron and soliton dynamics breaks down.

DOI: [10.1103/PhysRevB.73.024306](https://doi.org/10.1103/PhysRevB.73.024306)

PACS number(s): 63.20.Kr, 63.20.Ry, 41.20.Jb

I. INTRODUCTION

Many biological activities, such as photosynthesis, repair mechanism of DNA after radiation damage, metabolism, signal transduction in cells, enzymatic processes, and respiration are driven by electron transfer (ET) reactions.¹⁻⁴ In biomolecules ET is assumed to take place via a single-step tunneling over distances from donors to acceptors in the range of (5–20) Å, while the shortest time scale lies in the range of picoseconds. Characteristic for biomolecules is that they exhibit a strong interplay between function and structure. In fact, structural elements such as the protein backbone can serve as effective molecular wires along which electrons tunnel between redox sites in proteins. So has it been shown that in certain protein ET systems the electron tunneling occurs along polypeptide strands with tunneling jumps via hydrogen bonds.⁵⁻⁷ Moreover, recently, it has been demonstrated that typical biological systems ET may proceed along a single pathway which, as the preferred channel for ET, can be established by a hydrogen-bonded strand within the secondary structure.^{8,9}

The experimental evidence that polypeptide chains can form an effectively one-dimensional molecular wire appears to be highly promising for applicable molecular electronics offering a way to miniaturization on the nanoscale.¹⁰⁻¹³ From the perspective of using biomaterials in molecular electronics, the control of the electron flow is essential for the successful operation of electronic devices on the molecular scale. Such an achievement requests a theoretical under-

standing of the underlying transfer mechanism.

Theories on a molecular basis gave insight into the relation between the structure and function for charge and energy transfer in proteins.^{14,15} In particular, it was demonstrated that the H bridges contained in the protein structure play a crucial role for mediating ET. In fact, the dynamics of the bonds of proteins may serve as the driving force of ET.¹⁶

Attempts to theoretically describe the charge transport invoked from the beginning polaron and soliton models utilizing the idea that the interaction between the charge carrier and vibrational degrees of freedom of the molecular system conspire to form localized compounds.¹⁷ Assuming that a large width of the corresponding localized pulse compared to the spacing of the underlying lattice system shows that the continuum approximation can be applied and Davydov and co-workers showed that a mobile self-trapped state can travel as a solitary wave along the molecular structure.^{17,18} Later Davydov generalized the idea of solitonic exciton transport to include also charge transport in proteins.^{17,19,20} The soliton's stability is the result of the attained balance between two competing mechanisms, namely the interaction between an excitonic degree of freedom and the lattice vibrations of a polypeptide chain and, on the other hand, the lattice dispersion. The lattice vibrations are represented by acoustic phonon modes of a not too large amplitude allowing for their description in the harmonic approximation. However, to obtain higher velocities of the self-trapped compound necessitates larger lattice deformations so that the validity of the harmonic approximation does not hold anymore. Thus anhar-

monicity has to be included in the description of the lattice vibrations either by adding higher-order terms to the harmonic potential or considering from the beginning potentials with strong repulsive parts, represented by, e.g., Morse potentials.²¹ In the latter case, the lattice dynamics itself supports supersonic solitons which can accommodate charge and excitonic energy establishing transfer beyond the subsonic regime.^{22–27} Indeed, it has been proposed that supersonic acoustic solitons can capture and transfer self-trapping modes in anharmonic one-dimensional systems.^{23–26} In Ref. 23 it has been demonstrated that the supersonic quasiparticle transfer in a chain with anharmonic phonon part is achievable. In recent works^{24–26} the coupling between a quasiclassical electron dynamics and solitonic excitations in lattices with exponential repulsion has been studied. It has been shown that under special conditions the electrons might be trapped by the solitonic excitations due to the nonlinear lattice deformations. Further a nonlinear current-voltage characteristics has been derived. In other recent works^{28–34} anharmonic electron-lattice models have been studied in focusing on the inclusion of anharmonic effects in the multiphonon potential energy only and treating the coupling between the electron and the phonons harmonically. However, when larger displacements play a role the coupling term ought to include higher-order terms in the amplitude of the lattice vibrations as well. In the current work we consider a general form of an electron-vibration coupling term with exponential dependence originating from a distance dependence of the electronic transfer matrix element.

More precisely, we study a biomolecular ET chain model where we show that ET can be mediated by supersonic solitons using realistic parameter values of biomolecular systems. The model represents a typical one-dimensional polypeptide chain where neighboring peptide groups are bridged via hydrogen bonds (as it, for example, arises in the secondary structure of α -helix and β -sheet forms of proteins). We suppose that the hydrogen-bond pathway is the dominant one for ET in such a model protein and thus we focus our interest on ET along a one-dimensional channel consisting of a strand of hydrogen-bonded molecules.

Alternatively, the one-dimensional ET chain model can be regarded as a synthetically produced polypeptide chain built up from hydrogen-bridged peptides which may form the constituents, that is molecular wires, of a nanoscale electronic device.

With a view to possible applications in molecular electronics it is highly desirable to determine also the thermal stability of the soliton motion. For this aim the polymer lattice model, viz. the electronic tight-binding system coupled with longitudinal vibrations of the molecular units, is brought in contact with a heat bath. We focus our interest on whether the stable long-range soliton motion persists under the imposed thermal perturbations. Another aspect of our study is the influence of an applied electric field on the current produced by the electron soliton propagation.

The paper is then organized as follows: In the Sec. II we introduce our model for the polypeptide chain and recall the range of realistic parameter values for proteins. In Sec. III the soliton solutions are considered. Two methods are used to obtain them. First there is the possibility of launching them

“directly” in a lattice region by choosing proper initial values for the electron and lattice components in the form of localized states. It is demonstrated that these solitons accomplish long-range ET in the polypeptide chain. Alternatively, soliton solutions are constructed with the help of a variational approach with which lowest energy configurations are found that consist of a localized electron state and its assigned lattice deformation. Subsequently, we study the thermal stability of solitons. To this end the lattice system is coupled to a heat bath modeled by a stochastic force in the form of Gaussian white noise. The influence of an applied electric field on the soliton propagation is discussed in Sec. V. Finally, we give a summary of our results.

II. THE POLYPEPTIDE CHAIN MODEL

We study a linear lattice of molecules coupled by Morse forces in which one excess electron is imbedded. Accordingly, our model of charge transport in the system is based on the following Hamiltonian consisting of two parts:

$$H = H_{el} + H_{lattice}. \quad (1)$$

H_{el} describes quantum-mechanically the ET over the molecules in tight-binding approximation and $H_{lattice}$ represents the classical dynamics of longitudinal vibrations of the molecules, viz. stretchings and compressions of the associated H bonds. The electron dynamics and the coupling to the lattice are described by the tight-binding system

$$H_{el} = - \sum_n V_{n,n-1} (c_n^* c_{n-1} + c_n c_{n-1}^*). \quad (2)$$

The index n denotes the site of the n th molecule on the strand of hydrogen-bonded units and $|c_n|^2$ determines the probability to find the electron (charge) residing at this site. $V_{n,n-1}$ is the transfer matrix element (its value is determined by an overlap integral) being responsible for the nearest-neighbor transport of the electron along the chain.

The lattice part of the Hamiltonian, $H_{lattice}$, models dynamical longitudinal changes of the equilibrium positions of the molecules yielding alterations of the length of a hydrogen bond. The latter can appropriately be modeled by Morse potentials.^{27–35} The Hamiltonian of the $H_{lattice}$ is given by

$$H_{lattice} = \sum_n \left\{ \frac{p_n^2}{2M} + D \{ 1 - \exp[-B(q_n - q_{n-1})] \}^2 \right\}. \quad (3)$$

The coordinates q_n quantify the displacements of the molecules from their equilibrium positions along the molecular axis. D is the break-up energy of a hydrogen bond, B is the stiffness of the Morse potential, and M denotes the mass of a molecular unit. The Morse potential exhibits an exponential-repulsive part preventing the cross-over of neighboring lattice particles (molecules) for large displacements. Note that, with an expansion of the exponential functions, one recovers in lowest order the harmonic limit used in solid state physics^{21,36,37} and taking into account higher-order terms anharmonic potentials. On the other hand, the Morse potential looks very much like the six-twelve Lennard-Jones potential.^{21,25}

The interaction between the electronic and the vibrational degrees of freedom is due to the modifications of the electronic parameters $V_{n n-1}$ by displacements of the molecules from their equilibrium positions. To be precise, the transfer matrix elements $V_{n n-1}$ are supposed to depend on the relative distance between two consecutive molecules on the chain in the following exponential fashion:

$$V_{n n-1} = V_0 \exp[-\alpha(q_n - q_{n-1})]. \quad (4)$$

The quantity α regulates how strong $V_{n n-1}$ is influenced by the distance $r_n = q_n - q_{n-1}$, or in other words it determines the coupling strength between the electron and the lattice system. On the other hand, the actual charge occupation has its (local) impact on the longitudinal distortion of the molecular chain. Note that the exponential form of the electron-lattice interaction accounts also for small or large displacements of the lattice units thus going beyond the range of harmonic interaction studied in Refs. 17, 20, 28–34, 38, and 39. The latter limiting case is recovered by keeping only the linear term in an expansion of the exponential function in Eq. (4), i.e., $V(r_n) = V_0(1 - \alpha r_n)$, which is justified only for small arguments αr_n . In fact, for arguments $\alpha r = -0.5$ the linear treatment falls already by 25% short of those of the simplest anharmonic form including the next-order expansion term, i.e., $V(r_n) = V_0[1 - \alpha r_n + 1/2(\alpha r_n)^2]$. Therefore, for a more realistic description of stronger lattice deformations it is inevitable to include also higher-order contributions of the vibrational amplitudes in the electron-vibration interaction potential. We remark that in our model for a small coupling $\alpha/B = 1$ displacements of the order of $r_n = -0.78$ are encountered. For a coupling $\alpha/B = 1.75$ the maximal compression takes on the value $r_n = -1.54$.

For a dimensionless representation we introduce the following time scale: $\tilde{t} = \Omega_{Morse} t$, with $\Omega_{Morse} = \sqrt{2DB^2/M}$ being the frequency of harmonic oscillations around the minimum of the Morse potential. The energy of the system is then measured in units of the depth of the Morse potential, i.e., $H \rightarrow H/(2D)$. The dimensionless representation of the remaining variables and parameters of the system follows from the relations:

$$\tilde{q}_n = B q_n, \quad \tilde{p}_n = \frac{p_n}{\sqrt{2MD}}, \quad \tilde{V} = \frac{V_0}{2D} \quad (5)$$

$$\tilde{\alpha} = \frac{\alpha}{B}. \quad (6)$$

In what follows we drop the tildes.

The equations of motion derived from the Hamiltonian given in Eqs. (2) and (3) read as

$$i \frac{dc_n}{dt} = -\tau \{ \exp[-\alpha(q_{n+1} - q_n)] c_{n+1} + \exp[-\alpha(q_n - q_{n-1})] c_{n-1} \} \quad (7)$$

$$\begin{aligned} \frac{d^2 q_n}{dt^2} = & [1 - \exp\{- (q_{n+1} - q_n)\}] \exp[- (q_{n+1} - q_n)] \\ & - [1 - \exp\{- (q_n - q_{n-1})\}] \exp[- (q_n - q_{n-1})] \\ & - \alpha V \{ (c_{n+1}^* c_n + c_{n+1} c_n^*) \exp[-\alpha(q_{n+1} - q_n)] \\ & - (c_n^* c_{n-1} + c_n c_{n-1}^*) \exp[-\alpha(q_n - q_{n-1})] \}. \end{aligned} \quad (8)$$

The adiabaticity parameter $\tau = V/(\hbar \Omega_{Morse})$, appearing in the right-hand side of Eq. (7) determines the degree of time scale separation between the (fast) electronic and (slow) acoustic phonon processes.

With regard to parameter values we note that the geometrical parameters of the equilibrium configuration of hydrogen-bonded chains of biomolecules are well known.⁴⁰ The equilibrium length a of a hydrogen bond is in the range 3.4–5 Å, the dissociation energy is (0.04–0.3) eV and the range parameter $B \sim (2-5) \text{ \AA}^{-1}$. As the coupling strength between the electronic and lattice system is concerned, acceptable values for ET along hydrogen-bonded polypeptide chains can be obtained using values for the electron-phonon coupling strength from the Davydov model for charge transport in α -helices.^{17,20} Regarding charge transport along hydrogen-bonded chains for the value of the transfer matrix element holds $V_0 \leq 1.0 \text{ eV}$.^{18,20}

For our model study we use, unless stated otherwise, the following values representative of a typical H-bond chain: $a = 4 \text{ \AA}$, $D = 0.1 \text{ eV}$, $B = 4.45 \text{ \AA}^{-1}$, and $V_0 = 0.1 \text{ eV}$.^{2,3,40} For our computations we have chosen a value of the transfer matrix element V_0 lying one order of magnitude below the value used by Davydov in the context of solitary electron transfer in proteins.^{18,20} Nevertheless, with our choice of the value of V_0 a fairly pronounced time scale hierarchy between the fast electron and the slow vibrations is ensured. In fact, the characteristic frequencies are given then by $\Omega_{Morse} = 5.34 \times 10^{12} \text{ s}^{-1}$ and $\Omega_{electron} = V_0/\hbar = 1.52 \times 10^{14} \text{ s}^{-1}$ yielding an adiabaticity parameter $\tau = 28.47$. The influence of a larger transfer matrix element on the ET is currently being studied. The adjustable coupling parameter varies in the range $\alpha = (1-1.75)B$.

III. SOLITON PROPAGATION

A. Soliton launching

In order to generate soliton solutions of the coupled system we use two methods. First there is the possibility of launching a Toda-like soliton on the chain of coupled Morse oscillators. Indeed, in the range of parameter values relevant for the present study, the Morse chain exhibits compressions and localization features that are very similar to those of a Toda chain.^{25,41–43} Particularly, the Toda soliton solution which was expressed in appropriate units reads as

$$\exp[-\delta(q_n - q_{n-1})] = 1 + \beta^2 \cosh^{-2}(\kappa n - \beta t), \quad (9)$$

is preserved in the Morse chain with the soliton parameters $\delta \approx 3$ and $\beta = \sinh \kappa$ apart from the emission of small-amplitude waves. The latter radiation yields additional but negligibly small deformation of the molecular lattice chain. Moreover, as shown in Ref. 44 it is possible that a localized

electronic pulse travels in unison with the Toda soliton along the lattice chain accomplishing in this manner solitonic charge transport.

In order that this collective propagation takes place the initial electronic wave pattern has to match the shape of the Toda soliton according to

$$c_n(t) = \beta \cosh^{-1}[\kappa n - \beta t] \exp[-i(\omega t - \delta n + \sigma)], \quad (10)$$

with (angular) frequency

$$\omega = -2 \cos \delta \cosh \kappa, \quad (11)$$

and phase $\delta \in [-\pi, \pi]$. In the case of vanishing coupling $\alpha = 0$, the electron Eq. (7) is linear and hence, the localized pulse given in Eq. (10) disperses in the course of time. However, for $\alpha > 0$ an effective nonlinearity is induced in the electron equation and the latter gets the structure similar to the integrable the Ablowitz-Ladik's (AL) equation⁴⁵ which possesses soliton solutions. With the initial condition for the electron wave function, given in Eq. (10), it is assured that the Toda soliton and the localized electron pulse, in the form of a AL-soliton solution, travel concertedly along the lattice.

For the present study we have utilized this approach to excite solitonic charge transport in the coupled electron lattice-vibration system. We integrated with the help of a fourth-order Runge-Kutta method the set of coupled Eqs. (7) and (8) associated with a molecular lattice chain consisting of 99 sites where we imposed periodic boundary conditions. (An odd number of lattice sites was chosen to place the localized electronic occupation probability symmetrically at the central lattice site. However, whether the number of lattice sites is even or odd does not play a role so long as the length of the lattice is sufficiently large compared to the width of the localized electronic pulse.) The norm conservation $\sum_n |c_n(t)|^2 = 1$ (as well as the conservation of the total energy in the conservative case) was monitored during the integration procedure to guarantee accurate computations.

The spatiotemporal evolution of the electron and the lattice soliton, respectively, is presented in a density plot in Fig. 1 for strong coupling $\alpha = 1.75$. The energy contents attributed to the lattice deformation, that is the ‘‘phonon dressing’’ of the soliton, and the electron-phonon interaction are 0.0938 eV and -0.1306 eV, respectively, resulting in a soliton binding energy of -0.0368 eV (see also further below in Sec. III B). We emphasize that throughout this time no significant energy redistribution takes place, viz., the two subsystems virtually retain their allocated energy which proves also the dynamical stability of the soliton propagation.

Both the electron and lattice components move directionally along the lattice maintaining practically their respective localized structure apart from the emission of a small-amplitude wave from the main lattice deformation soliton. The solitons travel with velocity $v_{\text{soliton}} = 1.028v_s$ where v_s is the velocity of sound in the Morse chain. Thus supersonic, long-range and stable solitonic ET is achieved. We emphasize that the extension of the localized electron pulse is comparatively large which facilitates its motion.

B. Variational approach

As an alternative to the above described method solitons can also be obtained with the use of a variational approach. Again we seek for solutions where the lattice part is given by a Toda-like soliton. We consider solutions moving in a frame with $u = \kappa n - \beta t$ the traveling wave argument of the Toda soliton. The system for the spatial pattern can be obtained from the total energy of the system

$$E = \sum_n \left\{ \frac{1}{2} (1 - \exp[-\tilde{q}_n - \tilde{q}_{n-1}])^2 - V \exp[-\alpha(\tilde{q}_n - \tilde{q}_{n-1})] \right. \\ \left. \times (\phi_n^* \phi_{n-1} + \phi_n \phi_{n-1}^*) \right\}, \quad (12)$$

according to

$$\frac{\partial E}{\partial \tilde{q}_n} = 0, \quad \frac{\partial}{\partial \phi_n} \left(E + \omega \sum_n \phi_n^2 \right) = 0, \quad (13)$$

where the ϕ_n 's solve the corresponding stationary Schrödinger equation obtained from Eq. (7) with the substitution $c_n(t) = \phi_n \exp(-i\omega t)$ and where ω is the corresponding spectral parameter. The adiabatic approach is based on the fact that there is a large time scale hierarchy between the fast charge transport and the slow bond vibrations. In this case the inertia in Eq. (8) are negligible so that the energy of the system is given by Eq. (12).

Solutions of the Morse chain are supposed to be of the form of the Toda-soliton

$$\exp[-(\tilde{q}_n - \tilde{q}_{n-1})] = 1 + \sinh^2 \kappa \cosh^{-2}(\kappa n), \quad (14)$$

where κ is treated as a variational parameter. For the localized electronic solution we use a simple trial function

$$\phi_n = A \eta^{|n|}, \quad (15)$$

where the variational parameter $0 < \eta < 1$ gives the width of the solution. The closer η is to the value $\eta \rightarrow 1$ the more delocalized the state becomes. Correspondingly, for $\eta \rightarrow 0$ the state gets more localized. The coefficient A follows from the normalization condition and is evaluated as

$$A = \sqrt{\frac{1 - \eta^2}{1 + \eta^2}}. \quad (16)$$

The total variational energy is then given by

$$\Gamma = \frac{1}{2} \sum_n \frac{\sinh^4 \kappa}{\cosh^4(\kappa n)} - 2V \frac{1 - \eta^2}{1 + \eta^2} \\ \times \sum_n \left(1 + \frac{\sinh^2 \kappa}{\cosh^2(\kappa n)} \right)^\alpha \eta^{|n|} \eta^{|n-1|}. \quad (17)$$

For a given set of system parameters α and V the global minimum of Γ , giving the lowest energy configuration, has to be found in the two-parameter space (κ, η) . Unlike the above used ‘‘direct’’ method, for which in order to comply with the norm conservation the parameter κ is fixed to a single value, the present one has the advantage that it is also applicable to different values of κ resulting in various localized electron and lattice patterns.

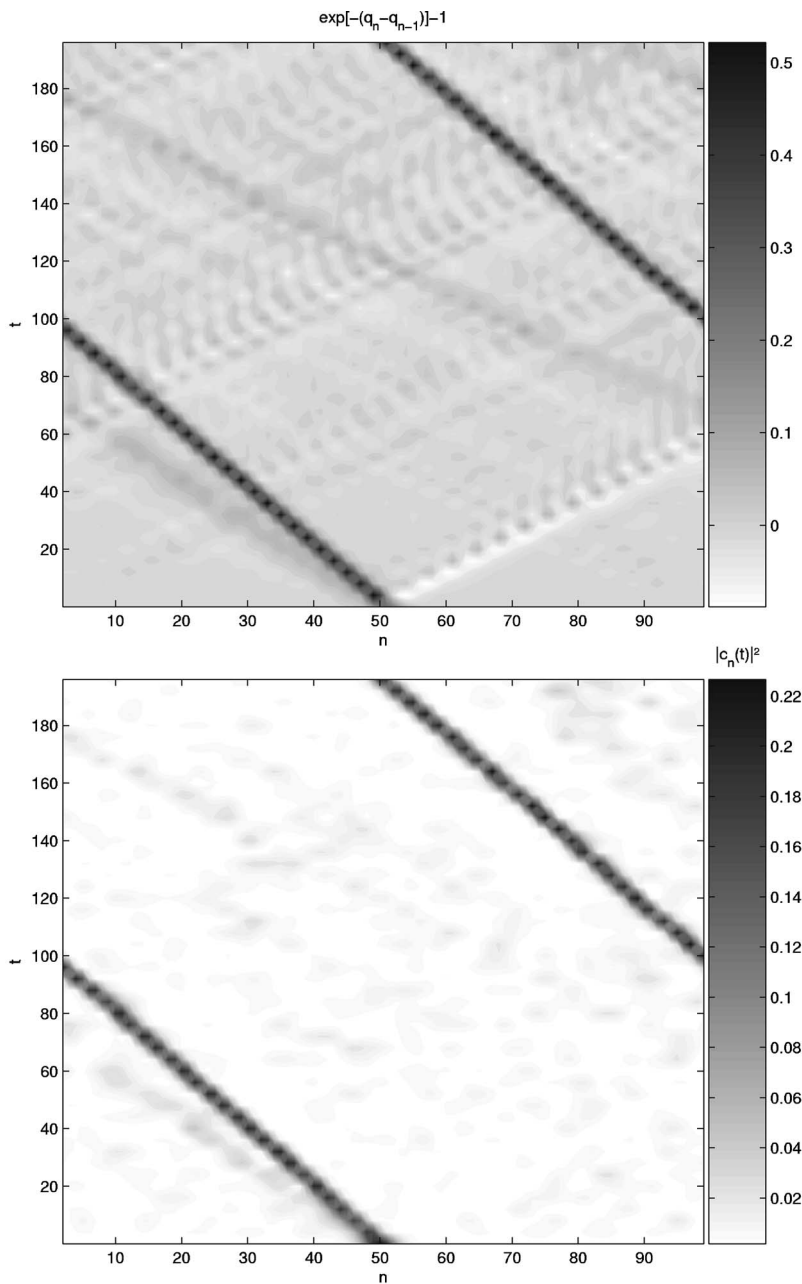


FIG. 1. Morse lattice. Density plot of the spatiotemporal evolution of the solitons with $\alpha = 1.75$. The amplitudes corresponding to the different colors is given in the panel at the right-hand side of the plots. (a) Lattice deformation $\exp\{-(q_n(t) - q_{n-1}(t))\} - 1$. (b) Electronic occupation probability $|c_n(t)|^2$.

In Fig. 2 we depict the localized pattern belonging to the ground state of the coupled system for three different coupling strengths. The electronic wave function is localized around a lattice site and the envelope of the amplitudes decays monotonically and exponentially with growing distance from this central site. The localized lattice pattern adapts a kinklike (domain wall or topological soliton) shape attributed to compression of the chain.²⁵ Likewise the electronic component of the ground state of the associated longitudinal displacement pattern, when represented in the form $\exp[-(q_n - q_{n-1})] - 1$, is bell-shaped, and is also exponentially localized around the central lattice site. With increased coupling strength, α , the width of the localized electronic pulse diminishes and the amplitude becomes higher and hence, the degree of electronic localization is enhanced. There is a smooth transition from a fairly extended electron pulse, ranging over

17 lattice sites, to a narrow state being localized at only four sites. Remarkably, as it will be illustrated further below, even the strongly localized states move along the lattice, a fact that distinguishes soliton solutions from their polaron counterparts, which are mobile only if their size is large enough to overcome the pinning effects of the lattice.^{46,47} Stronger localization of the electron demands larger binding energy which means higher deformation energy of the chain, meaning that the compression of the chain has to be suitably large. The binding energy of the soliton, E_b , is determined by Eq. (12). E_b measures the lowering of the energy of the system with respect to the lower band edge of the extended state. There is a growth of the binding energy with raising α ranging from $E_b = -0.2051$ eV for $\alpha = 1$ to $E_b = -0.2480$ eV for $\alpha = 1.75$. The binding energy has to be supplied externally in order to destroy the soliton. Consequently, in the dynamical

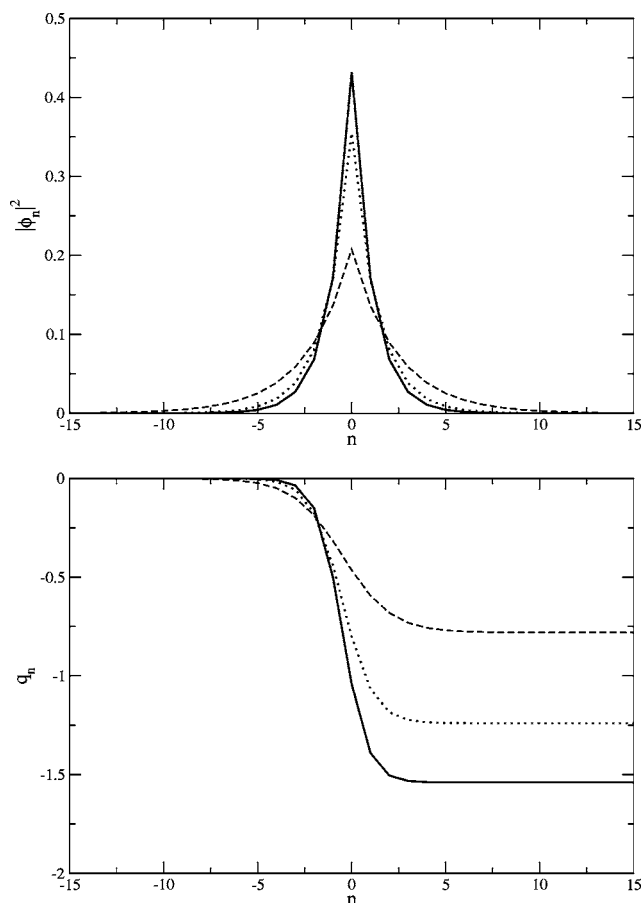


FIG. 2. Morse lattice. Spatial patterns of the localized states for different coupling strengths α . The assignment of the line types is as follows: dashed line, $\alpha=1.0$; dotted line, $\alpha=1.50$; and solid line, $\alpha=1.75$. (a) The electronic occupation probability $|\phi_n|^2$. (b) The longitudinal displacements q_n .

regime, the larger the coupling strength the more robust the solitons should be with regard to perturbations. The region of the lattice that has been traversed by the soliton remains in distorted shape for which the displacement of the corresponding lattice units from their equilibrium position is given as $\sim 2\kappa$ and for destruction of the soliton these units have to be brought back to their equilibrium positions.^{17,20} As the degree of the compression of the lattice is concerned we remark that for $\alpha=1$ ($\alpha=1.75$) the relative reduction of the length of a hydrogen bond is 4.27% (9.00%). The momentum of the lattice soliton with the corresponding value of κ is given by

$$p_n = 2\beta(\exp[2\kappa(n-1)]/\{1 + \exp[2\kappa(n-1)]\} - \exp[2\kappa n]/(1 + \exp[2\kappa n])). \quad (18)$$

The lattice soliton serves as the carrier of the localized electron pulse inducing in this manner a bound state (soliton). This is different from the above used direct method for soliton launching. In the latter case the electron pulse takes the actively part (even though the formation of the electronic AL soliton is induced by the coupling to the lattice Toda-soliton) for it possesses already initially its own momentum whereas

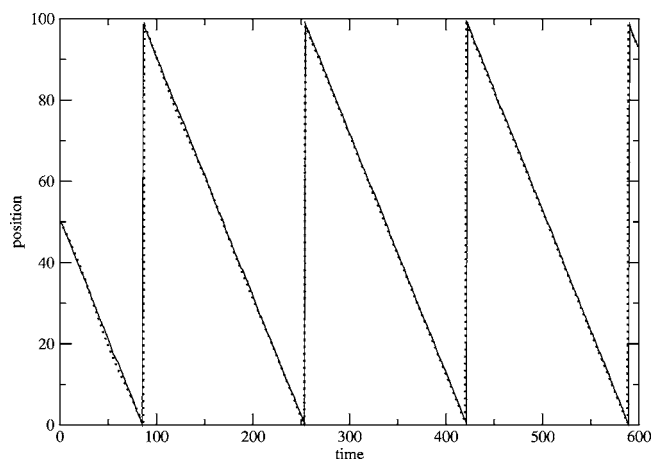


FIG. 3. Morse lattice. Time evolution of the first momentum of the electronic occupation probability (solid line) and of the lattice soliton (dotted line) defined in Eqs. (19) and (20), respectively. Parameter value: $\alpha=1.5$.

in the present case the initial electron wave function is represented by a standing wave (see also [Ref. 23]).

For characterization of the soliton propagation we plot in Fig. 3 the time evolution of the first momentum of the electronic occupation probability and that of the lattice deformation pattern defined as

$$\bar{n}_{electron}(t) = \sum_n n |c_n(t)|^2, \quad (19)$$

$$\bar{n}_{lattice}(t) = \sum_n n [\exp(-\{q_n(t) - q_{n-1}(t)\}) - 1]^2, \quad (20)$$

giving the position of the soliton. The coupling parameter is $\alpha=1.5$ giving an electron that is localized over five sites. Clearly, the supersonic electron and lattice soliton travel collectively with uniform velocity, $v_{soliton}=1.0653v_s$, corresponding to $v_s=12.361 \text{ \AA}/\text{ps}$, on the chain. In this manner the electron travels faster over long distances exceeding by far easily the maximal possible distance of 20 \AA achieved by a single-step tunneling.^{48,49}

Furthermore, the degree of localization of the electron and lattice energy can be measured using the partition number defined as

$$P_{electron} = 1 / \sum_n |c_n(t)|^4, \quad (21)$$

$$P_{lattice} = \sum_n E_{lattice}^2(t) / \left(\sum_n E_{lattice}(t) \right)^2, \quad (22)$$

respectively. Since the electronic wave function is normalized the electron is completely confined at a single site if $P_{electron}=1$ and is uniformly extended over the lattice if $P_{electron}$ is of the order N , viz. the number of lattice sites. Hence, $P_{electron}$ measures how many sites are excited to contribute to the electronic pattern. Equivalent arguments hold for $P_{lattice}$. We observed that both $P_{electron}$ as well as $P_{lattice}$ keep their initial value with negligible oscillatory variations around them.

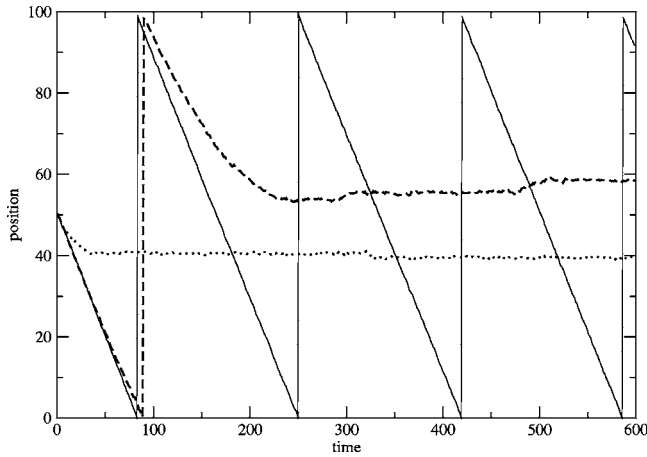


FIG. 4. Morse lattice. Temporal behavior of the position of the soliton on the lattice for different coupling strengths α . The line types are assigned as follows: solid line, $\alpha=1.6$; dashed line $\alpha=1.65$; dotted line $\alpha=1.75$.

With respect to the influence of the coupling strength α we remark that for couplings up to $\alpha \leq 1.6$ the motion is coherent, that is the solitons travel with constant velocity over long periods of time (in the simulation taken as 600 time units corresponding to ~ 112 ps). This behavior is presented in Fig. 4 depicting the time evolution of the first momentum of the electronic occupation probability for different α 's. When the coupling is increased the solitons still travel but with progressing time they become slower and eventually the motion terminates at a site at which the solitons stay from now on. Even for a large value $\alpha=1.75$, for which the size of the soliton is small (see Fig. 2), propagation is achieved in an initial phase. The soliton passes ten lattice sites, corresponding to a distance of 40 Å, before the motion terminates and the soliton gets trapped. That the motion of narrow electron and lattice solitons is accomplished at all is in so far remarkable as in the Holstein⁵⁰ and the Davydov model where the small polaron and soliton solutions, respectively, are immobile due to their pinning to the discrete lattice.^{17,20,33,46}

To illuminate how vital anharmonicity contained in the lattice vibration potential as well as the electron-lattice coupling is for the mobility of strongly localized states we compare our soliton solutions with those obtained in systems with harmonic interaction between a quasiparticle and the lattice vibrations, such as, e.g., the Holstein and Davydov system. To this end we have constructed strongly localized polaron states (located at five sites) in the Holstein system by adjusting a sufficiently strong coupling between the (intramolecular) optical vibrational mode and the electron. Attempts to initiate afterwards the motion of the standing polarons utilizing the method outlined in Ref. 51 failed. According to this method the motion is activated through suitable perturbations of the momentum variables in the direction of the so-called pinning mode. However, even for very strong perturbations (though beyond the physical energy range characteristic for excitations in the Holstein system) the polarons remain strictly immobile.

Regarding the Davydov system it seems not justified to construct exciton states which are localized over only a few

lattice sites on the basis of the mere *harmonic* coupling between the exciton and an (intermolecular) acoustic mode of the lattice. To obtain narrow exciton states fairly strong coupling to the lattice vibrations is necessary which in turn, as argued above, yield big amplitudes of the pulse of the lattice compressions. Therefore, the linear approximation in the lattice amplitude of the coupling term alone is no longer sufficient. Notice that the supersonic transport in the context of the Davydov model in Ref. 23 is demonstrated for two-component soliton solutions whose excitonic parts are fairly broad and the lattice compressions are comparatively strong but yet not too pronounced to hinder mobility.

Finally, let us note that we obtain qualitatively equal results when the value of the parameters a , b , D , and V_0 are varied in their respective ranges given above.

IV. THERMAL STABILITY

In this section we investigate the thermal stability of the soliton motion and hence the robustness of the charge transport. For this aim the system is brought in contact with a heat bath mimicked by a stochastic force acting upon the lattice and a corresponding damping. The corresponding Langevin equation reads as

$$\begin{aligned} \frac{d^2 q_n}{dt^2} = & [1 - \exp\{- (q_{n+1} - q_n)\}] \exp[- (q_{n+1} - q_n)] \\ & - [1 - \exp\{- (q_n - q_{n-1})\}] \exp[- (q_n - q_{n-1})] \\ & - \alpha V \{ (c_{n+1}^* c_n + c_{n+1} c_n^*) \exp[- \alpha (q_{n+1} - q_n)] \\ & - (c_n^* c_{n-1} + c_n c_{n-1}^*) \exp[- \alpha (q_n - q_{n-1})] \} - \gamma \frac{dq_n}{dt} \\ & + \sqrt{2D_b} \xi. \end{aligned} \quad (23)$$

We focus our interest on whether the stable long-range soliton motion persists under the imposed thermal perturbations. The stochastic term $\xi(t)$ on the right-hand side of Eq. (23) is of Gaussian white noise with zero mean and delta correlation, i.e., $\langle \xi(t) \rangle = 0$ and $\langle \xi(t) \xi(t') \rangle = \delta(t - t')$. The strength of the damping γ on the right-hand side of Eq. (23) is related to the amplitude of the stochastic force via the fluctuation-dissipation theorem, $D_b = k_B T \gamma / M$. The damping constant lies in the range $\gamma \leq 0.02$ corresponding to “life times” on time scales of at least 10 ps relevant for biological ET. As Fig. 5, illustrating the position of the solitons, reveals that the stable long-range soliton motion persists under the imposed thermal perturbation even at temperature $T=300$ K for which $E_B = -0.2245$ eV is considerably above $k_B T$. For small enough damping parameters $\gamma_c \leq 0.01$ the thermal perturbations effectively do not have an impact on the soliton propagation of the zero temperature regime although in the end the solitons become a little bit slower. For a critical damping strength $\gamma > \gamma_c$ the motion of the solitons is characterized by an initial phase during which propagation is still achieved albeit with gradual reduction of the velocity with progressing time so that finally, the soliton gets trapped at a lattice site. Apparently, the departure of the electron from the original coherent soliton path is more pronounced the stronger the γ .

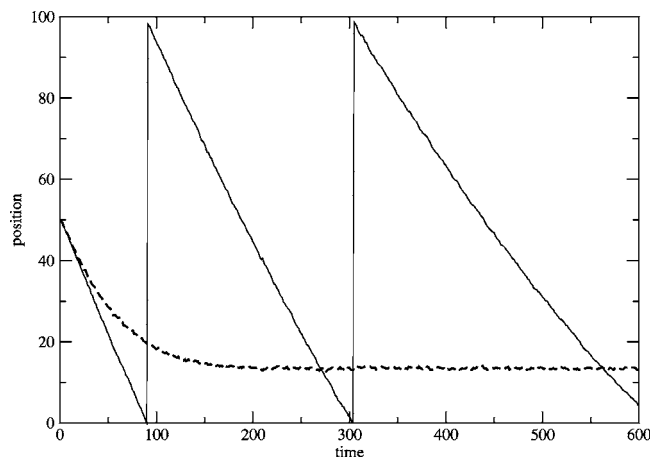


FIG. 5. Morse lattice. Time evolution of the first momentum of the electronic occupation probability at $T=300$ K and for damping $\gamma=0.002$ (solid line) and $\gamma=0.02$ (dashed line). Parameter value: $\alpha=1.5$.

Nonetheless, in the entire γ -interval, that is physically relevant, the solitons are able to travel over a distance of at least 35 consecutive lattice units during the phase of maintained soliton propagation before they come to a halt. Moreover, we note that the solitons keep their localized patterns throughout the time, a behavior which is reflected in the corresponding evolution of the partition numbers which exhibit small-amplitude oscillations around the mean value determined by the initial partition number. Similar features regarding thermal stability of solitons were found for the Davydov model.^{20,52–54}

Interestingly, in cases of relatively weak couplings, i.e., $\alpha \leq 1.2$, the decoupled lattice soliton alone, when subjected to thermal fluctuations, gets destroyed. The thermal sensitivity of the lattice soliton is due to the fact that the lattice deformation energy is then simply too low compared to $k_B T = 0.024$ eV at $T=300$ K. Nevertheless, the bound combination of the solectron persists even for small electron-vibration couplings. This illustrates that the resulting binding energy of the soliton is far below the lower edge of extended states to assure its thermal stability.

V. ELECTRIC FIELD

Finally, we studied also the role of an electric field on the electron propagation. To this aim the right-hand side of the electron equation is modified by an additional term according to

$$i \frac{dc_n}{dt} = -\tau \{ \exp[-\alpha(q_{n+1} - q_n)] c_{n+1} + \exp[-\alpha(q_n - q_{n-1})] c_{n-1} \} - n \tilde{E} c_n, \quad (24)$$

with the dimensionless field strength $\tilde{E} = ea / (\hbar \Omega_{\text{Morse}}) E$. As shown in the preceding section for sufficiently small damping γ the soliton evolution remains virtually unaltered (even at temperature $T=300$ K). Thus, focusing interest on the impact of the electric field on the soliton dynamics, we can

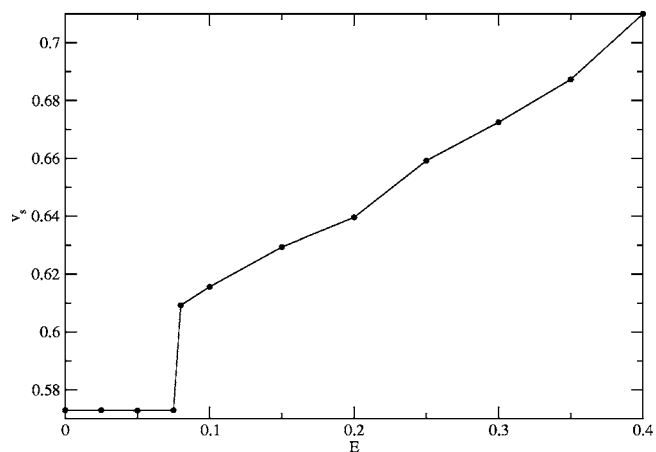


FIG. 6. Morse lattice. The velocity of the solectron as a function of the strength of the electric field. One unit on the abscissa is equivalent to $0.879 \cdot 10^5$ V/cm while one unit on the ordinate corresponds to 21.428 Å/ps.

restrict the current study to the $T=0$ case. Furthermore, since for small damping the relaxation time of the (damped) lattice motion is considerably larger than our simulation time the lattice vibration proceeds virtually frictionless. The dynamics is initialized with soliton solutions gained with the help of the variational method described in Sec. III B. We apply an electrical field acting in the direction of the running soliton. We study how the interaction between the running soliton and the moving electron influences the electron flow. Our results are summarized as follows: For low field strengths E smaller or equal to $E_c \leq 0.0738 \times 10^5$ V/cm the solectron propagation is independent of the electric field and the velocity, and thus the current is always that of the field-free case. For field strengths above E_c there exists an interval in which the current follows Ohm's law, viz. the soliton travels with a constant velocity that is proportional to E . Interestingly, the soliton propagation proceeds in each case, i.e., with and without the external field, with constant velocity hinting that the kinetic energy allocated to the soliton stays unaltered (see also Ref. 55). These features are illustrated in Fig. 6 depicting the velocity of the solectron as a function of the field strength. Eventually, for large values $E \geq 3.518 \times 10^5$ V/cm soliton dissociation occurs, viz. under the action of the strong field the electron is immediately swept over the lattice without being accompanied by its lattice counterpart anymore. For strong fields the heavy lattice particles are too sluggish to adjust rapidly enough to follow the fast electron motion imposed by the field.⁵⁶ Clearly, if we proceed from high field values down at $E=E_c$ there is a transition from Ohmic to non-Ohmic electric conduction (see also Ref. 26).

VI. SUMMARY

In the present paper we have investigated the soliton mediated propagation in a hydrogen-bonded chain model in the realm of the charge transfer in biomolecular chains. The corresponding model system comprises two parts, a tight-binding system accounting for the description of the quantum-transport of a charged entity (an excess electron or

hole) along the lattice sites (molecular units) and a Morse chain modeling the displacement of the molecules from their equilibrium positions along the molecular axis, viz. the stretchings and/or compressions of the hydrogen bonds. The coupling between the electronic and lattice vibrations is due to the dependence of the electronic transfer matrix element on the relative distance between two neighboring molecules in an exponential fashion. This renders the electron-vibration coupling to be of anharmonic type going beyond the usually considered harmonic coupling. We have focused interest on the excitation of soliton solutions in the chain which accomplish long-lived and stable charge transfer. To this end two methods have been employed. First, choosing properly shaped initial conditions, solitons are directly launched in the lattice yielding a two-compound soliton solution containing the localized charge pattern together with its attributed lattice deformation. Concerning the Morse chain the solitonic wave is of the form of a Toda soliton constituting a domain wall (topological soliton) that leaves the region that has been traversed by it permanently distorted, i.e., the associated hydrogen bonds remain compressed. The bell-shaped electronic wave function travels in unison with the lattice deformation with supersonic velocity.

Alternatively, we have invoked a variational approach to construct a soliton in the Morse chain and electronic tight-binding lattice, respectively, composing so a soliton state of the coupled electron-vibration system (the solectron). The stronger the electron-vibration coupling the higher is the degree of localization of the solitons. Strikingly, even movement of narrow electron states, being localized mainly on five lattice sites, is supported by the supersonic solitons. It has been demonstrated that for realistic parameter values, being representative for strands built up from hydrogen-bonded peptides, the solitons travel over long distances maintaining their localized shape. Hence, the pinning effect due to the discreteness of the underlying lattice is subdued. This feature differentiates the solectron with the foundation on anharmonic lattice-vibrations and corresponding electron-vibration interaction from their counterparts that exist in the Holstein and Davydov model, respectively, relying on the harmonic exciton vibration interaction. In the latter two cases the corresponding polaron and soliton solutions, respectively,

are mobile only if their width is large enough to overcome the pinning barrier of the lattice. On the other hand, our findings lead us to the conclusion (of some universal validity) that with anharmonic vibrations supersonic carriers can promote the transport of narrow excitations. This result is also valid when due to dissipation the soliton must be maintained by an appropriate input-output energy balance.²⁶

Furthermore, we have investigated the impact of thermal perturbations on the soliton propagation and hence the robustness of the solectron. For this scope the lattice system is brought into contact with a heat bath that is mimicked by a Gaussian white noise with zero mean, and delta-function correlations. The corresponding damping constant is related to the temperature via the fluctuation-dissipation theorem. Altogether the evolution of the solitons virtually does not change under the impact of thermal perturbations because the soliton binding energy exceeds always the thermal energy for all couplings $1 \leq \alpha \leq 1.75$. As for the influence of the damping constant we have found that for values $\gamma \geq 0.01$ the directed soliton motion prevails in an initial phase but at last there occurs soliton trapping impeding further motion. Nevertheless, even in the strong damping case the ET takes place on biologically relevant time scales and the charge is carried over fairly long distances.

Finally, we have studied the influence of an applied external electric field on the ET. For relatively high values of the field the velocity of the solitons is proportional to the field strength and hence, the associated current obeys Ohm's law. Lowering the field strength we have found a regime for which the soliton velocity is kept at a constant level independent of the field strength. For relatively higher values above a critical field strengths the solectron is ruptured with the consequence that the electron is swept over the lattice by the strong field.

ACKNOWLEDGMENTS

The authors wish to express their gratitude to Professors A. P. Chetverikov, G. Nicolis, P. Clavin, A. C. Scott, P. C. Hemmer, M. Alonso, and Dr. J. Porter for useful criticism and enlightening suggestions. This research was sponsored by the European Union under Grant No. SPARK FP6-004690.

¹D. DeVault, *Quantum-mechanical Tunneling in Biological Systems* (Cambridge University Press, Cambridge, U.K., 1984).

²J. A. McCammon and S. C. Harvey, *Dynamics of Proteins and Nucleic Acids* (Cambridge University Press, Cambridge, U.K., 1987).

³C. Branden and J. Tooze, *Introduction to Protein Structure* (Garland, New York, 1991).

⁴B. Alberts, D. Bray, J. Lewis, M. Raff, K. Roberts, and J. D. Watson, *Molecular Biology of the Cell* (Garland, New York, 1983).

⁵H. B. Gray and J. R. Winkler, *Annu. Rev. Biochem.* **65**, 537 (1996).

⁶A. A. Stuchebrukhov, *Adv. Chem. Phys.* **118**, 1 (2001).

⁷J. Kim and A. A. Stuchebrukhov, *J. Phys. Chem. B* **104**, 8606 (2000).

⁸I. A. Balabin and J. N. Onuchic, *J. Phys. Chem.* **100**, 11573 (1996).

⁹P. E. M. Siegbahn, M. R. A. Blomberg, and R. H. Crabtree, *Theor. Chem. Acc.* **97**, 289 (1997).

¹⁰J. J. Hopfield, *Proc. Natl. Acad. Sci. U.S.A.* **71**, 3649 (1974).

¹¹J. J. Hopfield, J. N. Onuchic, and D. N. Beratan, *Science* **241**, 817 (1988).

¹²A. Yu. Kasumov, M. Kociak, S. Gueron, B. Reulet, V. T. Volkov, D. V. Klinov, and H. Bouchiat, *Science* **291**, 280 (2001).

- ¹³M. Ratner, *Nature (London)* **397**, 480 (1999).
- ¹⁴D. N. Beratan, J. N. Onuchic, and J. J. Hopfield, *J. Chem. Phys.* **86**, 4488 (1987).
- ¹⁵J. N. Onuchic and D. N. Beratan, *J. Chem. Phys.* **92**, 722 (1990).
- ¹⁶M. H. Vos, M. R. Jones, C. N. Hunter, J. Breton, J.-C. Lambry, and J.-L. Martin, *Biochemistry* **33**, 6759 (1994).
- ¹⁷A. S. Davydov, *J. Theor. Biol.* **38**, 559 (1973); A. S. Davydov and N. I. Kislukha, *Sov. Phys. JETP* **44**, 571 (1973); A. S. Davydov, *Sov. Phys. Usp.* **25**, 898 (1982).
- ¹⁸A. S. Davydov, *Solitons in Molecular Systems* (Reidel, Dordrecht, 1985); *J. Theor. Biol.* **38**, 559 (1973).
- ¹⁹*Davydov's Soliton Revisited*, edited by P. L. Christiansen and A. C. Scott (Plenum, New York, 1991).
- ²⁰A. C. Scott, *Phys. Rep.* **217**, 1 (1992).
- ²¹Ph. Choquard, *The Anharmonic Crystal* (Benjamin, New York, 1967).
- ²²S. Yomosa, *Phys. Rev. A* **32**, 1752 (1985).
- ²³A. V. Zolotaryuk, K. H. Spatschek, and A. V. Savin, *Phys. Rev. B* **54**, 266 (1996).
- ²⁴M. G. Velarde, W. Ebeling, and A. P. Chetverikov, *Int. J. Bifurcation Chaos Appl. Sci. Eng.* **15**, 245 (2005).
- ²⁵A. P. Chetverikov, W. Ebeling, and M. G. Velarde, *Int. J. Bifurcation Chaos Appl. Sci. Eng.* (to be published).
- ²⁶A. P. Chetverikov, W. Ebeling, and M. G. Velarde, *Contrib. Plasma Phys.* **45**, 275 (2005).
- ²⁷A. P. Chetverikov, W. Ebeling, and M. G. Velarde, *Eur. Phys. J. B* **44**, 509 (2005).
- ²⁸B. G. Vekhter and M. A. Ratner, *J. Chem. Phys.* **101**, 9710 (1994); B. G. Vekhter and M. A. Ratner, *Phys. Rev. B* **51**, 3469 (1995).
- ²⁹J. K. Freericks, M. Jarrell, and G. D. Mahan, *Phys. Rev. Lett.* **77**, 4588 (1996).
- ³⁰S. Flach and K. Kladko, *Phys. Rev. B* **53**, 11531 (1996).
- ³¹Bin Zhou and Ji-Zong Xu, *J. Phys.: Condens. Matter* **10**, 7929 (1998).
- ³²Y. Zolotaryuk and J. C. Eilbeck, *J. Phys.: Condens. Matter* **10**, 4553 (1998).
- ³³N. K. Voulgarikis and G. P. Tsironis, *Phys. Rev. B* **63**, 014302 (2002).
- ³⁴D. Hennig, *Phys. Rev. E* **62**, 2846 (2000).
- ³⁵P. Morse, *Phys. Rev.* **34**, 57 (1929).
- ³⁶N. W. Ashcroft and N. D. Mermin, *Solid State Physics* (Holt, Rinehardt and Winston, Philadelphia, 1976).
- ³⁷C. Kittel, *Quantum Theory of Solids* (Wiley, New York, 1987).
- ³⁸P. L. Christiansen, J. C. Eilbeck, V. Z. Enol'skii, and Yu. B. Gaididei, *Phys. Lett. A* **166**, 129 (1992).
- ³⁹Yu. B. Gaididei, P. L. Christiansen, and S. F. Minaleev, *Phys. Scr.* **51**, 289 (1995).
- ⁴⁰L. Stryer, *Biochemistry* (Freeman, New York, 1995).
- ⁴¹M. Toda, *Phys. Rep.*, C **18**, 1 (1975).
- ⁴²M. Toda, *Theory of Nonlinear Lattices* (Springer-Verlag, Berlin, 1991).
- ⁴³J. Dunkel, W. Ebeling, U. Erdmann, and V. Makarov, *Int. J. Bifurcation Chaos Appl. Sci. Eng.* **12**, 2359 (2002).
- ⁴⁴D. Hennig, *Phys. Rev. E* **61**, 4550 (2000).
- ⁴⁵M. J. Ablowitz and J. F. Ladik, *J. Math. Phys.* **17**, 1011 (1976).
- ⁴⁶M. Peyrard and M. D. Kruskal, *Physica D* **14**, 88 (1984).
- ⁴⁷S. Flach and C. R. Willis, *Phys. Rep.* **295**, 181 (1998).
- ⁴⁸H. B. Gray and J. Halpern, *Proc. Natl. Acad. Sci. U.S.A.* **102**, 3533 (2005).
- ⁴⁹B. M. Sjöberg, *Struct. Bonding (Berlin)* **88**, 139 (1997).
- ⁵⁰T. Holstein, *Ann. Phys. (N.Y.)* **8**, 325 (1959).
- ⁵¹D. Chen, S. Aubry, and G. P. Tsironis, *Phys. Rev. Lett.* **77**, 4776 (1996).
- ⁵²W. Förner, *Phys. Rev. A* **44**, 2694 (1991).
- ⁵³W. Förner, *J. Phys.: Condens. Matter* **3**, 4333 (1991); **4**, 1915 (1991); **5**, 823 (1993); **5**, 3883 (1993); **5**, 3897 (1993).
- ⁵⁴L. Cruzeiro-Hansson, *Phys. Rev. Lett.* **73**, 2927 (1994).
- ⁵⁵Å. Johansson and S. Stafström, *Phys. Rev. Lett.* **86**, 3602 (2001); *Phys. Rev. B* **65**, 045207 (2002).
- ⁵⁶D. M. Basko and E. M. Conwell, *Phys. Rev. Lett.* **88**, 056401 (2002).